Received: 7 May 2017 | Accepted: 18 July 2018

DOI: 10.1111/1365-2435.13192

RESEARCH ARTICLE

Functional Ecology | BRITISH ECOLOGICAL SOCIETY

Population-level responses to temperature, density and clonal differences in *Daphnia magna* as revealed by integral projection modelling

Marjolein Bruijning | **Anne C. M. ten Berge** | **Eelke Jongejans**

Department of Animal Ecology and Physiology, Radboud University, Nijmegen, The Netherlands

Correspondence
Marjolein Bruijning, Department of Animal Ecology and Physiology, Radboud University, Nijmegen, The Netherlands.
Email: M.Bruijning@science.ru.nl

Handling Editor: Kwang Pum Lee

Abstract

1. Raising global temperatures are predicted to have strong consequences for ectotherms, as metabolic rates depend directly on external temperatures. To understand consequences for population fitness, a full life cycle approach is important because (a) temperature can have opposite effects on different vital rates (growth, survival, reproduction) and (b) sensitivities of population growth rate to changes in vital rates can vary in magnitude. As vital rates are concurrently influenced by other factors, adequately predicting temperature effects requires factors such as body size, population density and genetics to be taken into account.
2. The aim of this study was to quantify the role of temperature on all vital rates of *Daphnia magna* individuals and their integrated effects on population dynamics. In addition, we evaluated how clonal lineages differed in their temperature response, both on the vital rate and population level.
3. We performed a laboratory experiment, in which we followed 40 populations (five clonal lineages × eight temperatures) during 80 days. Due to our novel set-up, we were able to quantify vital rates of individuals within those populations. We identified relations between vital rates and body size, lineage, temperature and population density and used a size-structured integral projection model to integrate the experimental effects over all vital rates.
4. We found negative density dependence in growth and reproduction, resulting in lineage-specific carrying capacities. Population fitness showed a thermal optimum that differed among genotypes. It is interesting that we found that clones had different life-history strategies, optimizing population fitness via different routes. As no lineage outperformed the others in all vital rates, we identified trade-offs between vital rates, which had strong effects on the dynamics of the population. Moreover, simulations suggest that the genetic composition of mixed populations is temperature-dependent.
5. Our results underscore the importance of studying individuals within their population when predicting responses to environmental change. The observed density effects, which were as strong as temperature effects but explained considerably more variation in population growth, would have been overlooked in life table

experiments. Furthermore, differential temperature responses emphasize the importance of genetic variation in the ability of ectotherm species such as *Daphnia magna* to respond to climate change.

KEYWORDS
density dependence, integral projection models, integration across the life cycle, life-history strategies, population model, thermal tolerance, trade-offs, vital rates

1 | INTRODUCTION

Raising global temperatures are predicted to have strong consequences for ectotherms, as their metabolic rates directly depend on external temperatures (Huey & Berrigan, 2001). To avoid local extinction, populations must appropriately respond to these increasing temperatures, for instance by phenotypic plasticity or by evolution (Gienapp, Teplitsky, Alho, Mills, & Merilä, 2008; Hoffmann & Sgrò, 2011). However, disentangling plastic and evolutionary processes is not straightforward, and predicting their relative importance in natural populations is a major challenge (van Benthem et al., 2017; Chevin, Collins, & Lefèvre, 2013; Lavergne, Mouquet, Thuiller, & Ronce, 2010; Pelletier, Garant, & Hendry, 2009; Schoener, 2011).

To understand short-term environmentally induced changes in population dynamics, it is important to know how the performance of individuals within the population is affected, as it is the sum of the number of surviving individuals and number of newborns that determines the success of a population. Temperature effects on various life-history traits of ectotherms have been studied extensively, using for instance life table experiments (e.g. Carvalho, 1987; MacArthur & Baillie, 1929; Van Doorslaer, Stoks, Duvivier, Bednarshka, & De Meester, 2009). However, in addition to temperature, vital rates (growth, survival and reproduction) are shaped by many other factors, such as body size (Brooks, Mugabo, Rodgers, Benton, & Ozgul, 2016; Ozgul, Coulson, Reynolds, Cameron, & Benton, 2012), genotype (Dudycha & Tessier, 1999; Geerts et al., 2015) and population density (Guisande, 1993; Ozgul et al., 2012). The complex interplay between all these factors influences how individual plasticity and evolution will alter vital rates. Therefore, adequately predicting climate-driven changes in vital rates requires taking into account all these factors.

Integrating over all vital rates is a key element when studying eco-evolutionary dynamics (Smallegange & Coulson, 2013). Without doing so, the combined effect for the population remains unknown (McLean, Lawson, Leech, & Pol, 2016). This is because population-level effects do not only depend on the observed effect sizes of changes in vital rates, but also on the sensitivity of population growth rate to these vital rate changes (de Kroon, van Groenendael, & Ehrlén, 2000). Moreover, changes can have opposite effects in different life stages. Positive and negative (including trade-offs) correlations between vital rates exist (Stearns, 1989), and their net effects will be overlooked without integrating the effects over all life stages (Villellas, Doak, García, & Morris, 2015). For example, a widespread phenomenon among ectotherms is that at higher temperatures, individual development rates increase, but individuals tend to mature at a smaller body size (Atkinson, 1994, 1995; Kingsolver & Huey, 2008). Given that fecundity is often related to body size, temperature may result in life-history changes that have opposite effects on population growth. Hence, the estimation of the net population-level effects of this "temperature-size rule" requires integration over all life stages and multiple vital rates. Integral projection models (IPMs) are a powerful tool to integrate vital rates fitted to individual level data (Ellner, Childs, & Rees, 2016; Ellner & Rees, 2006) and have been used to study eco-evolutionary dynamics (e.g. Chevin, 2015; Coulson, MacNulty, Stahler, Wayne, & Smith, 2011; Ozgul et al., 2010; Traill, Schindler, & Coulson, 2014).

In this study, we use the water flea *Daphnia magna* as a study system. This species has been widely used in studies on genetics (Colbourne, Pfrender, & Gilbert, 2011), toxicology (e.g. Gust et al., 2016), as well as in studies on rapid evolution and eco-evolutionary dynamics (De Meester, Van Doorslaer, Geerts, Orsini, & Stoks, 2011; Hairston et al., 1999; Van Doorslaer et al., 2009, 2010). In addition, various factors have been shown to affect specific vital rates, such as effects of temperature (Henning-Lucass, Cordellier, Streit, & Schwenk, 2016), genetic background (Henning-Lucass et al., 2016; Pietrzak, 2011), food concentration (Gabsi, Glazier, Hammers-Wirtz, Ratte, & Preuss, 2014) and population density (Guisande, 1993). *Daphnia magna* individuals reproduce parthenogenetically when environmental conditions are favourable and switch to sexual reproduction when conditions worsen (Kleiven, Larsson, & Hobæk, 1992), which results in the production of long-lived dormant eggs. This has the advantage that asexual reproduction can be assured in the laboratory by keeping conditions favourable. Therefore, genetic variation can be controlled, and the same genotypes can be used across treatments.

Although there are multiple studies on eco-evolutionary dynamics in *D. magna*, we are not aware of any study quantifying the role of ecological and genetic factors on the success of a population of interacting individuals, via their integrated effects on reproduction and survival of all life stages (see Duchet, Coutellec, Franquet, Lagneau, & Lagadic, 2010; Sommer, Piscia, Manca, Fontaneto, & Ozgul, 2016, for parameterizations of a matrix population model based on isolated *Daphnia* individuals). Due to our novel set-up, we are able to follow individuals within their population, to explicitly quantify how population density affects vital rates, in addition to the effects of temperature and genotype.

The aim of this study was to quantify how temperature, genetic background and population density affect the dynamics of *Daphnia magna* populations, and through which vital rates. We do so by performing a laboratory experiment, exposing five clonal lineages to a temperature gradient (10–26°C) and following the populations for 80 days, while collecting both population-level and individual-level data. By identifying relations between body size and demographic processes, and combining them into an integral projection model, we aim to answer the following questions: (a) How does temperature affect vital rates of *D. magna* individuals within dynamic populations? (b) How do these effects on the individual level propagate to the population level? (c) How do clonal lineages differ in their vital rates and population-level responses, and can we identify trade-offs between vital rates? 4) What is the relative importance of temperature, compared to genetic background and population density, in shaping population dynamics?

2 | MATERIALS AND METHODS

2.1 | Clonal lineages

In June 2014, we extracted *Daphnia magna* dormant eggs from mud collected in a small lake in Hilversum (Laapersveld), the Netherlands. These eggs were stored in the dark at 4°C. From September 2014, we stimulated hatching by exposing the eggs to light and 20°C. The eggs were checked daily, and neonates were placed in individual 100-ml tubes, held in Dutch Standard Water (DSW; Hoefnagel, de Vries, Jongejans, and Verberk (2018)) (200 mg/L $CaCl_2.2H_2O$, 180 mg/L $MgSO_4.7H_2O$, 100 mg/L $NaHCO_3$, 20 mg/L $KHCO_3$; NEN6503 (1980)) and fed with instant algae (1.6×10^5 cells/ml; Shellfish 1800, Reed Mariculture). Medium, containing new food, was refreshed three times per week. In total, of the 50 dormant eggs, we established 22 lineages. Of these lineages, 12 were successfully kept alive until the beginning of the experiment, in December 2015. Four lineages were randomly chosen for the experiment. In addition, we included a *D. magna* lineage that had been successfully held in the laboratory for more than 10 years, originally also extracted from a lake in the Netherlands (Lürling & Tolman, 2010). This enabled us to specifically look at within-population variation as well as comparing dynamics to a lineage that has been known to perform well under laboratory conditions. In total, this resulted in five clonal lineages (A1-A4 indicating the newly collected lineages, L indicating the existing laboratory lineage). Note that lineages L, A3 and A4 are referred to as C, D and E, respectively, by Hoefnagel et al. (2018).

2.2 | Experimental set-up

The experiment was conducted in a climate chamber, with a 16:8-hr light:dark regime and temperature set at 18°C. We established a gradient of eight temperatures ranging between 10 and 26°C. We achieved the cooler temperatures by placing four basins containing demineralized water above each other and cooling the upper basin to 10°C using a water bath. Demineralized water was continuously pumped from the lowest basin to the upper basin. Using an overflow system, cold water continuously flowed from a basin to the one below it, slowly reaching chamber temperature (18°C), resulting in a gradient from 10 to 18°C. The same was done for the four warmer temperatures: The upper basin was heated to 26°C, and using a continuous overflow, a gradient was obtained. In this way, we generated a stable temperature gradient of eight temperatures: 10.5, 14.3, 15.5, 17.0, 20.0, 22.3, 23.5 and 25.9°C. Temperatures were constantly measured by temperature loggers. In each basin, we placed five 2-L aquaria, each aquarium containing one population of a different lineage (see Supporting Information Appendix S1 for a schematic drawing).

The experiment ran between December 1, 2015, and February 18, 2016, lasting 80 days. Prior to the experiment, individuals were placed in the experimental set-up for more than 3 weeks to acclimatize to their respective temperature treatments and to reduce differences due to maternal effects. Using eight temperatures and five lineages, this resulted in 40 experimental units. On Day 1, we arbitrary chose 20 individuals from each aquarium, reflecting the full range of body sizes (i.e. from small juveniles to adults), to start the experiment with. Every eight hours, an automatic pump system added 200 ml fresh DSW medium including instant algae (8×10^6 cells/ml) to each aquarium. Volume in each aquarium was held constant by an overflow system, as each aquarium contained a sieve (0.3 mm sieve size). For comparison, the smallest measured neonate was 0.67 mm, and 95% of the measured neonates were larger than 0.83 mm. Of all measured individuals, 95% was >0.97 mm.

We placed three transparent PVC tubes (4 cm diameter) in each aquarium, containing 12 holes (1 cm diameter) covered with permeable filters (0.125 mm sieve size; preventing neonates to escape or enter the tubes), allowing food and other cues to pass. These were used to isolate individuals for either three or 4 days, to obtain individual measurements, while ensuring that the individuals experienced the same environment as the rest of the population.

2.3 | Population counts

For each aquarium, measurements were taken twice per week; for half of the aquaria this was on Monday and Thursday, and for the other half on Tuesday and Friday. This resulted in a time interval of either three or 4 days. On these days, each population was transferred to a Petri dish, which was placed in a fixed camera set-up. A movie of approximately 4 s was made with a digital camera (Sony Handycam, HDR-CX115). We used newly developed R-package *trackdem* to obtain estimates of population counts (Bruijning, Visser, Hallmann, & Jongejans, 2018). In short, movies were converted into an image sequence and loaded in the R-environment (R Core Team 2016). As only individuals move, a background image was created, containing all motionless objects. By subtracting all images from this background, moving particles were detected. Identification was optimized using machine learning. Individual trajectories were subsequently reconstructed (Jaqaman et al., 2008). We obtained 20 counts for each of the 40 populations.

2.4 | Individual measurements

At the same time as the population counts, we collected data on individuals in the tubes, using a stereo microscope. We noted whether the individual was alive and measured its body size, as measured from the base of the spine until the middle of the eye. We counted the number of eggs in the brood pouch and noted the stage of the eggs (1: round, no eyes, 2: oval shape, 3: development of eyes and limbs) for 317 individuals, across all temperatures and lineages. If present, we counted the number of released (alive) offspring and measured the size of one of the neonates. All these individuals were joined with their respective population. The aquarium and tubes were rinsed with hot water, and we arbitrarily selected a new individual for each tube. These newly chosen individuals were also measured, and their number of eggs was counted. At last, all other individuals were placed back in the aquarium, and the aquarium was randomly positioned in the appropriate basin (using lists of random placements). This resulted in 2,293 observations of demographic rates (three individuals × five clones × eight temperatures × twice a week × 11 weeks of measuring; three populations went extinct early during the experiment, see "Results" section, explaining the discrepancy) over either a three- or four-day interval, providing information on size-dependent survival, growth, probability of carrying eggs, probability of reproduction, clutch size and neonate size (from now on called "vital rates") (Bruijning, ten Berge, & Jongejans, 2018).

2.5 | Explanatory variables

We explored population density effects on vital rates (Supporting Information Appendix S2) and found negative density dependence in growth and reproduction, and positive density dependence in survival. We therefore included density in regressions related to growth and reproduction. The apparent positive density dependence found for survival is addressed in Discussion. Prior to all analysis, we standardized body size, temperature and population size to enable a comparison of effect sizes. For regressions including lineage, we used lineage A1 as a reference category, and all other lineages as contrasts to A1.

2.6 | Model framework

Integral projection models (IPMs) describe the dynamics of a population in which individuals are characterized by a continuous state variable in discrete time (Ellner & Rees, 2006; Ellner et al., 2016). We used (standardized) body size z as the continuous state variable. The IPM consisted of four kernels, describing how z influences all vital rates.

We have constructed IPMs following four different procedures, with increasing complexity. IPM_1 was constructed using the collected data directly, describing transitions on an approximately 3.5-day basis. $IPM_{2\text{-}4}$ described daily transitions, requiring a translation of collected data (twice per week) to daily rates, as explained below. For notation, daily rates have subscript d. $IPM_{2\text{-}4}$ differed from each other in the reproduction kernel. For IPM_2, we divided estimated reproduction by 3.5, the average time interval. For IPM_3 and IPM_4, we used data on the egg stages to estimate temperature-dependent daily development rates and the average number of days it takes early-stage eggs to develop into neonates (Supporting Information Appendix S3 for more details). At last, IPM_4 was a size- and stage-structured model in which individuals were, in addition to body size, characterized by a discrete developmental stage of the eggs they carried. Here, we defined four discrete stages (1: round, no eyes, 2: oval shape, 3: development of eyes and limbs and 4: released neonates); individuals had to move through all stages before offspring was born and added to the population.

We here provide details and results for IPM_2. Because we preferred an IPM structure with a daily time step, we did not use IPM_1. $IPM_{2\text{-}4}$ used the same vital rates except for details on reproduction, but IPM_2 was the least complex. See Supporting Information Appendices S4–S5 for details and results of the other approaches, which were to a large degree similar to those of IPM_2.

The constructed IPM predicts the body size distribution at day $t + 1$ ($n(t + 1, z')$), given the body size distribution at day t ($n(t, z)$). The four kernels describing all daily transition probabilities were (a) survival $S_d(z)$, (b) growth $G_d(z'|z)$, describing probabilities for surviving individuals of size z at time t to obtain size z' at day $t + 1$, (c) reproduction $R_d(z)$ and (d) an offspring size distribution $D_d(z'|z)$ describing probabilities of obtaining offspring with size z' at $t + 1$ given a maternal size z at Day t. We created a composite IPM, whereby the four kernels were functions of, in addition to z, temperature T, observed population density N as estimated using *trackdem* (Bruijning, Visser, et al., 2018) (except for survival) and lineage C:

$$n(t+1,z') = \int [S_d(z,T,C)\cdot G_d(z'|z,T,N,C) + R_d(z,T,N,C)\cdot D_d(z'|z,T,N,C)]\, n(t,z)dz \quad (1)$$

Reproduction ($R_d(z, T, N, C)$) was defined as the product of the probability of carrying eggs (p), the probability of having live offspring at the end of a half-week interval conditional on carrying eggs (f) and clutch size at birth (L_0), divided by 3.5 to translate to daily estimates:

$$R_d(z,T,N,C) = p(z,T,N,C)\cdot f(z,T,N,C)\cdot L_0(z,T,N,C)\cdot \frac{1}{3.5} \quad (2)$$

Note that $p(z, T, N, C)$ and $f(z, T, N, C)$ do not have subscript d, as data did not need to be translated to obtain daily estimates. We translated observations on clutch size to predict clutch size at birth $L_0(z, T, N, C)$, as explained below.

New size distribution and offspring size distribution were functions of the size-dependent expected growth ($\hat{g}_d(z)$) and expected offspring size at birth ($\hat{\varphi}_0(z)$), respectively, and the estimated variation around these means (σ_g and σ_ϕ):

$$G_d(z'|z,T,N,C) = \text{Normal}[z'|\hat{g}_d(z,T,N,C),\sigma_g] \quad (3)$$

$$D_d(z'|z,T,N,C) = \text{Normal}[z'|\hat{\varphi}_0(z,T,N,C),\sigma_\phi] \quad (4)$$

The IPM was discretized into a 100 × 100 matrix, with (standardized) z ranging between −3 and 3, corresponding to 0.07 and 4.1 mm, respectively.

2.7 | Estimation of vital rates

The collected data on individuals were used to estimate all vital rates needed to parameterize the IPM kernels. For each vital rate, we tested all models including additive effects of body size z, temperature T, population density N and clonal lineage C. We also included a quadratic effect of z and T because visual inspection revealed nonlinear effects. At last, we included two-way interactions between z and T, z and C, C and T and C and N. The most complex model was thus:

$$y(z,T,N,C) = \beta_0 + \beta_1 z + \beta_2 T + \beta_3 N + \beta_4 z^2 + \beta_5 T^2 + \beta_6 zT + \sum_{i=1}^{4} (\beta_{6+i} C_i + \beta_{10+i} zC_i + \beta_{14+i} TC_i + \beta_{18+i} NC_i) + \epsilon_{res} \quad (5)$$

Here, C_i is clone i ($A2$, $A3$, $A4$ or L); effects of clone i are compared to those for clone $A1$. We fitted all 196 models nested within this model. Instead of choosing the best model based on AIC, we applied model averaging (based on AIC weights) over all models to obtain averaged parameters and standard errors using the R-package *MuMIn* (Bartoń, 2016; Burnham & Anderson, 2002), after ensuring that explanatory variables were only weakly correlated ($r^2_{T-N} = 0.039$, $r^2_{z-N} = 0.00029$, $r^2_{T-z} = 0.028$). We chose to perform model averaging because this results in more robust models, where there is model uncertainty (reflected by similar AIC values across different models). Model averaging has been shown to improve prediction accuracy and reduce the risk of finding spurious effects (e.g. Burnham & Anderson, 2004; Hoeting, Madigan, Raftery, & Volinsky, 1999; Lukacs et al., 2010; Madigan & Raftery, 1994; Raftery, Madigan, & Hoeting, 1997; Yang, 2007). We used the conservative zero method for averaging coefficients, in which parameters are assigned a zero if not present in a model (Grueber, Nakagawa, Laws, & Jamieson, 2011). In the case of a log or logit link function, averaging coefficients may yield different results than averaging predictions, but differences were negligible in our case (see Supporting Information Appendix S6). The procedure for each vital rate will now be explained.

2.8 | Survival probability

As time intervals between measurements varied, we estimated survival as a function of time between measurements (in days; Δt):

$$\left[\frac{1}{1+\exp\left(k\left(z,T,C\right)\right)}\right]^{1/\Delta t} = S_d\left(z,T,C\right)^{1/\Delta t} \quad (6)$$

Here, $k(z, T, C)$ is the linear relation between the explanatory variables (Equation 5). To calculate the exact time interval (Δt), we used the time at which the population was filmed. Intervals ranged between 2.8 and 3.2 days and between 3.8 and 4.2 days. We optimized a likelihood function to fit $S_d(z, T, C)$. In accordance with the other vital rates, we tested all different models and performed model averaging based on AIC.

2.9 | Growth

To fit daily growth $\hat{g}_d(z, T, N, C)$, individual growth was first calculated by dividing observed size increment by the time interval (Δt), assuming that growth rates were constant within these days. Daily growth was then fit as a linear function of size, temperature, density and lineage. Growth variation σ_g was calculated as the standard deviation of the residuals.

2.10 | Probability of carrying eggs

We only included individual measurements when they were placed in the tube (i.e. not using individual measurements 3 or 4 days later) to avoid pseudoreplication caused by repeated measurements. We dichotomized the number of eggs in the brood pouch into zeros (0 eggs) and ones (>0 eggs). By performing a logistic regression and model averaging, we fitted $p(z, T, N, C)$.

2.11 | Probability of producing offspring

We included all individuals carrying eggs at Day 1 (i.e. the day when they were placed into the tubes). Individuals that produced neonates when remeasured were assigned ones, other individuals were assigned zeros. These binomial data were used to fit probability of producing offspring after, on average, 3.5 days, $f(z, T, N, C)$, conditional on carrying eggs, using logistic regression.

2.12 | Clutch size

To estimate clutch size at birth $L_0(z, T, N, C)$, we took into account that born offspring (observed when remeasuring the parent) could have been born 0–4 days earlier. To do so, we first used $\hat{g}_d(z, T, N, C)$ to predict neonate body sizes 0, 1, 2, 3, 4 days earlier, based on neonate size when measured (and relevant temperature, density and lineage). Second, we predicted survival probabilities for each day, given predicted body sizes, using $S_d(z, T, C)$. For all days, the probability of surviving until the measurement was calculated, by multiplying probabilities with probabilities of consecutive days. Afterwards, observed clutch size was divided by each of these probabilities. This gave the expected clutch size, if offspring would have been born on that day, given the observed clutch size and given expected survival probabilities. We assumed equal birth probabilities for each day and averaged these predicted clutch sizes. We log-transformed these estimates and fitted clutch size at birth $L_0(z, T, N, C)$, using linear regression.

2.13 | Neonate body size at birth

A similar procedure was followed to estimate neonate body size at birth $\hat{\varphi}_d(z, T, N, C)$. We used the fitted growth function ($\hat{g}_d(z, T, N, C)$) to

back-calculate the sizes 0–4 days earlier. Assuming equal birth probabilities for each day, we took the average of these numbers as an estimate for offspring body size at birth. Estimates were fit as a function of maternal size, temperature, density and lineage. We calculated the standard deviation of residuals to estimate variation in estimated offspring body size σ_ϕ.

2.14 | Integrated effects of temperature and density

The fitted vital rates were used to quantify the population-level effects of the temperature and density, using an IPM (Equation 1). To evaluate how temperature and density effects in single vital rates propagated to the population, we performed the following analyses: First, we calculated temperature effects on projected (asymptotic) population growth rate (λ), which is the dominant eigenvalue of the discretized IPM. To do so, we constructed an IPM for temperatures ranging between 9 and 28°C, for each lineage, and calculated λ. Here, we set N at 0, that is average density (corresponding to 96 individuals). Second, density effects (at average temperature, 18.6°C) were calculated by varying density between one individual and the maximum lineage-specific density across all temperatures. We calculated λ for each density and lineage. Third, we analysed how much of the variation in projected population growth rate was explained by variation in temperature, lineage and density. We used each of the observed population sizes during the experiment and projected λ based on an IPM with the corresponding lineage, temperature and density, resulting in 915 growth rates. A linear regression was performed between λ and T (and T^2), C or N, and we calculated coefficients of determination (R^2) for each of these three regressions.

2.15 | Population-level consequences of lineage differences

We quantified the population-level consequences of lineage differences in single vital rates. We started by calculating the average IPM among all lineages, by taking the average matrix for a specific temperature (λ_T). Afterwards, we systematically replaced one of the vital rates (averaged across lineages) by the vital rates of each lineage and recalculated λ. The difference between λ_T and λ when one of the vital rates is replaced combines the effect size and the sensitivity of λ to that vital rate. This was done for temperatures ranging between 9 and 28°C. To evaluate within-population differences, we performed the same analysis excluding lineage L, which originated from a different population.

2.16 | Quantifying uncertainty in population growth rates

We used bootstrapping to obtain measures of uncertainty in population growth rates. Per population, we resampled individual observations from the dataset, with replacement. This way we created 500 bootstrapped datasets. Vital rate models were fitted, and IPMs were constructed as described above for each of the 500 datasets. We performed all above-described analysis with the constructed IPMs, that is lineage-specific temperature and density effects, and how differences in vital rates between lineages propagated to the population level.

2.17 | Simulating dynamics of a hypothetical mixed population

At last, we used IPMs to simulate a scenario in which lineages were mixed in one population, to explore whether the genetic composition is predicted to be temperature-dependent. We simulated density-dependent dynamics with all lineages starting with four 1.7 mm individuals, which is the average observed body size (i.e. standardized body size set at 0). For each time step, we constructed a density- and temperature-dependent IPM per lineage, using the total density across all lineages. We projected population size, per lineage, at $t + 1$ by matrix multiplying the appropriate IPM with the lineage-specific population structure at time t. Populations were projected for 100 days, and this analysis was performed for temperatures between 9 and 28°C. At Day 100, for each temperature, the lineage composition was evaluated. To focus specifically on within-population clones, this analysis was also performed without lineage L.

3 | RESULTS

3.1 | Population trends

Thirty-seven of the 40 populations remained viable during the 80 days of the experiment. Three populations of lineage A4 (at 17, 22.3 and 25.9°C) went extinct after 10 days. After acclimatization, we restarted these populations with 20 individuals on Day 49, from which they remained viable until Day 80. Most populations started with an initial increase, although the rate and timing of that increase differed between temperatures and lineages (Supporting Information Appendix S7). The populations fluctuated considerably in size over time, with a maximum number of 500 individuals (for lineage L at the lowest temperature, after 40 days).

3.2 | Vital rates

For all vital rates, estimated rates are shown for lineage A1, average density and both the highest (25.9°C) and the lowest (10.5°C) temperatures (Figure 1). See Supporting Information Appendix S8 for estimated vital rates per temperature.

3.3 | Survival

The best model (having 67% of the weight) describing daily survival included an effect of size, squared size, temperature, lineage and an interaction between size and temperature (Supporting Information Tables S2, S8–S9 in Appendix S9). Survival probabilities showed an optimum for medium sizes and lower survival at higher temperatures (β_4, β_2 in Table 1; Figure 1a), as well as a negative interaction between size and temperature (β_6), such that survival was further

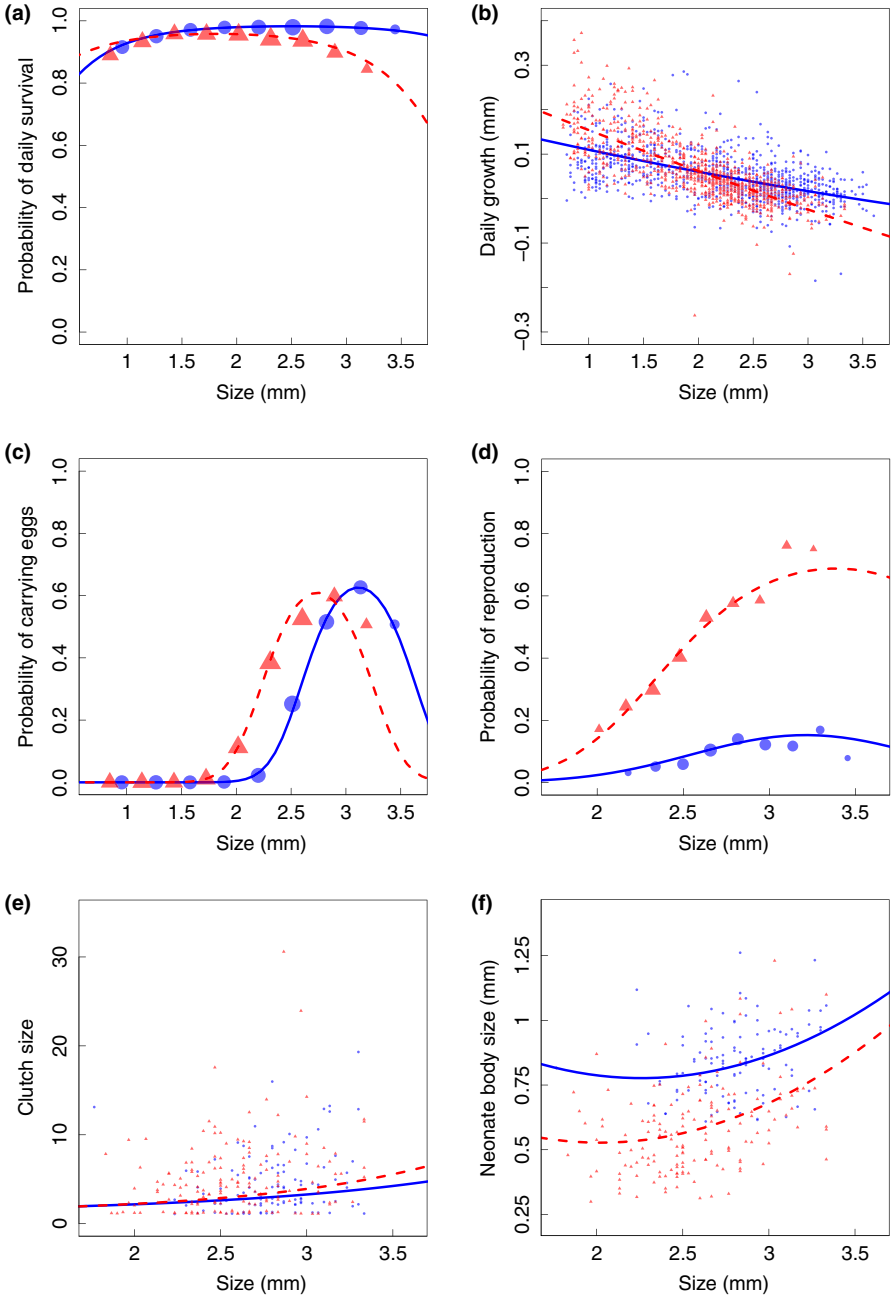

FIGURE 1 Estimated vital rates, shown for lineage A1 at high temperatures (25.9°C; red dotted lines) and low temperatures (10.5°C; blue solid lines), according to the full averaged model (fitted across all temperatures and linages) (coefficients in Table 1). Note that the six intermediate temperatures fall between the shown model predictions for the lowest and highest temperatures. In a), daily survival probability $S_d(z, T, C)$; (b), daily growth $g_d(z, T, N, C)$; (c), probability of carrying eggs $p(z, T, N, C)$; (d), probability of reproduction $f(z, T, N, C)$; (e) clutch size $L_0(z, T, N, C)$; and (f), neonate body size $\varphi_0(z, T, N, C)$. All predictions are shown for lineage A1 and for average population density. Dots represent partial residuals, which plot the residuals around the two plotted lines of size-dependent model predictions. We separately did so for the four highest temperatures (red triangles around the red lines) and for the four lowest temperatures (blue circles around the blue lines). Those show the density of observations over all body sizes, irrespective of density, lineage or temperature. In (a), (c) and (d), partial residuals are averaged per size class, and dots are scaled to the number of data points

reduced at higher temperatures for larger animals. Parameters β_2, β_4, β_6 were all significant in both the averaged model and in the best model (Table 1, Supporting Information Table S8). Lineage A2 had highest and lineage A3 the lowest daily survival probabilities ($\beta_{7\text{-}10}$).

3.4 | Growth

Daily growth $\hat{g}_d(z, T, N, C)$ was on average 0.058 mm (for lineage A1, body size, density and temperature all set at their mean) and decreased with body size (β_1; Figure 1b). The best model (17% of the weight) included effects of size, squared size, density, lineage, temperature, squared temperature and interactions between size and lineage, and size and temperature (Supporting Information Tables S3, S9). A negative interaction between temperature and size was found (β_6; Figure 1a), suggesting that at higher temperatures, individuals initially grew faster, but stop growing at a smaller size. The cumulative sum of the AIC weights for main effects of size, temperature, density and genetic lineage was 1.00 for each of these variables, as well as a size x temperature interaction. All averaged coefficients that differed significantly from zero were also significant according to the best model (Table 1, Supporting Information S10–S11). Variation in growth (σ_g) equalled 0.048.

3.5 | Carrying eggs

Probability of carrying eggs $p(z, T, N, C)$ equalled practically zero for individuals of up to 1.5 mm and increased with size (β_1; Figure 1c). Temperature had a positive effect on estimated probabilities (β_2),

TABLE 1 Weighted coefficients and standard errors for each of the vital rates, daily survival probability $S_d(z, T, C)$, daily growth $G_d(z, T, N, C)$, probability of carrying eggs $p(z, T, N, C)$, probability of reproduction $f(z,T, N, C)$, clutch size at birth $L_0(z, T, N, C)$ and neonate body size at birth $\phi_0(z, T, N, C)$. Bold numbers indicate significant effects ($p < 0.05$). The following linear regression was used for each vital rate (but with different link functions; see main text): $y\left(z,T,N,C\right) = \beta_0 + \beta_1 z + \beta_2 T + \beta_3 N + \beta_4 z^2 + \beta_5 T^2 + \beta_6 zT + \sum_{i=1}^{4} (\beta_{6+i} C_i + \beta_{10+i} zC_i + \beta_{14+i} TC_i + \beta_{18+i} NC_i) + \varepsilon_{res}$

		$S_d(z, T, C)$	$G_d(z, T, N, C)$	$p(z, T, N, C)$	$f(z, T, N, C)$	$L_0(z, T, N, C)$	$\phi_0(z, T, N, C)$
	βo	**3.45e+00 [1.02e-01]**	**5.82e-02 [3.27e-03]**	**−2.72e+00 [3.27e-01]**	**−2.24e+00 [5.26e-01]**	2.57e-01 [2.35e-01]	**−2.15e+00 [8.32e-02]**
z	β_1	4.55e-02 [4.04-02]	**−4.59e-02 [2.51e-03]**	**5.31e+00 [5.58e-01]**	**2.20e+00 [9.52e-01]**	**5.01e-01 [1.80e-01]**	−1.52e-02 [8.45e-02]
T	β_2	**−2.65e-01 [4.91e-02]**	−6.90e-04 [1.97e-03]	**9.32e-01 [2.14e-01]**	**6.10e-01 [2.24e-01]**	1.96e-02 [1.33e-01]	**−1.20e-01 [6.10e-02]**
N	β_3		**−6.45e-03 [3.07e-03]**	−2.50e-01 [1.77e-01]	**−7.67e-01 [3.84e-01]**	−8.42e-02 [1.25e-01]	1.20e-02 [2.36e-02]
z^2	β_4	**−2.92e-01 [4.11e-02]**	1.26e-03 [1.42e-03]	**−2.14e+00 [2.58e-01]**	−6.04e-01 [4.83e-01]	9.99e-03 [6.84e-02]	**1.07e-01 [2.70e-02]**
T^2	β_5	1.04e-02 [1.10-02]	−1.32e-03 [1.45e-03]	-1.19e-01 [9.10e-02]	−7.48e-02 [1.11e-01]	−2.49e-03 [5.57e-02]	−8.33e-05 [1.14e-02]
zT	β_6	**−1.88e-01 [4.00e-02]**	**−9.02e-03 [1.31e-03]**	**−7.60e-01 [1.69e-01]**	9.96e-02 [2.22e-01]	4.16e-02 [1.11e-01]	2.41e-02 [3.57e-02]
C	β_7	**5.67e-01 [1.50e-01]**	**−1.24e-02 [3.79e-03]**	−7.81e-02 [3.71e-01]	3.27e-01 [5.03e-01]	−3.93e-01 [3.76e-01]	**2.68e-01 [1.01e-01]**
	β_8	**−2.40e-01 [1.21e-01]**	−4.30e-03 [3.71e-03]	**1.03e+00 [3.89e-01]**	−7.48e-02 [4.84e-01]	1.47e-01 [2.47e-01]	−7.55e-03 [8.76e-02]
	β_9	−9.24e-02 [1.32e-01]	4.64e-03 [3.89e-03]	5.51e-02 [4.16e-01]	**1.14e+00 [4.61e-01]**	9.94e-02 [2.51e-01]	5.27e-02 [1.45e-01]
	β_{10}	5.45e-03 [1.29e-01]	−6.85e-03 [3.55e-03]	**1.83e+00 [3.99e-01]**	6.94e-01 [3.76e-01]	1.05e-01 [2.32e-01]	1.65e-01 [1.10e-01]
zC	β_{11}	−8.41e-04 [3.05e-03]	7.77e-03 [4.23e-03]	−1.40e-01 [3.94e-01]	8.13e-02 [3.59e-01]	5.33e-03 [7.93e-02]	−8.37e-02 [9.56e-02]
	β_{12}	−3.37e-03 [3.88e-03]	1.69e-03 [3.49e-03]	−3.42e-01 [4.12e-01]	−4.65e-03 [1.83e-01]	−6.75e-03 [8.33e-02]	−5.19e-02 [7.66e-02]
	β_{13}	−2.78e-03 [3.54e-03]	6.40e-04 [3.58e-03]	2.98e-01 [4.17e-01]	1.62e-02 [2.07e-01]	−3.48e-03 [1.02e-01]	−1.39e-01 [1.41e-01]
	β_{14}	6.35e-05 [2.55-03]	−4.44e-03 [3.85e-03]	−5.45e-01 [5.37e-01]	−1.94e-02 [1.94e-01]	1.06e-02 [9.46e-02]	−1.29e-01 [1.22e-01]
TC	β_{15}	2.02e-02 [3.92-02]	−1.97e-05 [1.76e-03]	**−6.15e-01 [2.55e-01]**	−3.81e-03 [6.49e-02]	1.63e-03 [7.13e-02]	5.00e-02 [7.72e-02]
	β_{16}	−3.97e-02 [4.55e-02]	1.87e-03 [3.65e-03]	−2.72e-01 [2.29e-01]	1.54e-03 [5.32e-02]	1.41e-02 [9.22e-02]	2.67e-02 [5.13e-02]
	β_{17}	−5.48e-02 [5.75e-02]	6.64e-04 [2.21e-03]	−1.06e-01 [2.08e-01]	−2.05e-03 [5.63e-02]	1.05e-02 [7.97e-02]	3.49e-03 [3.95e-02]
	β_{18}	2.66e-02 [3.83-02]	1.06e-03 [2.61e-03]	**−5.34e-01 [2.56e-01]**	3.53e-03 [5.61e-02]	−4.97e-03 [6.82e-02]	3.50e-02 [6.14e-02]
NC	β_{19}		2.74e-03 [4.38e-03]	−1.85e-01 [2.35e-01]	3.26e-01 [4.52e-01]	−3.53e-03 [5.83e-02]	−7.24e-04 [1.30e-02]
	β_{20}		−3.44e-04 [3.15e-03]	−4.90e-01 [4.32e-01]	−4.46e-01 [5.84e-01]	−4.63e-03 [7.41e-02]	−9.87e-04 [1.62e-02]
	β_{21}		3.50e-04 [2.95e-03]	−8.58e-02 [2.38e-01]	4.28e-01 [5.04e-01]	−2.24e-04 [5.44e-02]	−5.70e-04 [1.31e-02]
	β_{22}		2.04e-03 [3.61e-03]	−1.94e-02 [1.85e-01]	5.70e-01 [5.15e-01]	2.55e-03 [5.69e-02]	−1.91e-03 [1.79e-02]

and this effect was significant in both the averaged and best model (Table 1, Supporting Information Table S12). For the largest individuals, probabilities started decreasing as reflected by the significant negative squared size effect (β_4), in both the averaged and best model. Significant lineage effects were found ($\beta_{7\text{-}10}$). At last, density had a negative effect on the probability, although insignificant

in the averaged and best model. The best model (with 32% of the weight) was the full model, including all additive effects and interactions (Supporting Information Tables S4, S12–S13). Cumulative AIC weights for main effects of size, temperature, density and genetic lineage, and interactions between size and temperature, equalled 1.00.

3.6 | Probability of producing offspring

The best model (17% of the weight) describing included all additive effects, as well as the interactions between lineage and density (Supporting Information Tables S5, S14–S15). The cumulative sum of the AIC weights was 1.00 for main effects of size, temperature and density, and 0.97 for genetic lineage. Probabilities $f(z, T, N, C)$ increased with temperature and body size ($\beta_{1\text{-}2}$ in Table 1; Figure 1d), and lineage A4 showed significant higher probabilities compared to lineage A1 (β_9). A significant negative effect of density was found (β_3). All significant coefficients were present, and significant, in the best model (Table 1, Supporting Information Table S14).

3.7 | Clutch size at birth

Number of offspring $L_0(z, T, N, C)$ increased with size (β_1; Figure 1e; significant in both the averaged and best model, see Table 1, Supporting Information Table S16–S17). At higher temperatures, slightly higher clutch sizes were reached, but temperature effects were insignificant and the cumulative sum of the AIC weights of models including main effects of temperature was 0.57. Differences in AIC values were small, indicating that there was support for a wide range of models (Supporting Information Table S6).

3.8 | Neonate body size distribution at birth

Predicted neonate body size at birth averaged 0.80 mm for a mother of 3 mm (for lineage A1 and all other variables set at 0) and increased with maternal squared size (β_4; Figure 1f; significant in both the averaged and best model, see Table 1, Supporting Information Table S18–S19). Temperature had practically no effect and lineage A2 produced significant (in both the averaged and full model) larger offspring compared to lineage A1 (β_7). Again, differences in AIC were small, indicating support for a wide range of models (Supporting Information Table S7), although the cumulative sum of AIC weights including main effects of temperature, genetic lineage and squared body was, equalled 1.00 for each of these variables. Variation in offspring size σ_ϕ equalled 0.25.

3.9 | Integration over all vital rates

We here report the results using estimates of daily vital rates to construct IPM_2. Results from daily based IPM_3 and IPM_4 are similar and do not change our conclusions. IPM_1, describing transitions after one measurement interval (on average 3.5 days), gave more divergent results (more details and results in Supporting Information Appendix S4–S5).

3.10 | Effects of lineage, temperature and density

We found that lineage, temperature and density all affected asymptotic population growth rate (λ) (Figure 2; Supporting Information Appendix S10). In general, lineage L showed the highest λ across all temperatures, with rates above 1 for up to almost 400 individuals. At average density, it is only at the lowest temperatures that lineage A4 showed slightly higher growth rates. Although all lineages showed a wide thermal optimum within the range of tested temperatures, this optimum differed between lineages (Figure 2a). Population growth rate of lineage A2 started decreasing more rapidly with increasingly high temperatures, whereas lineage L outperforms the other lineages in particular at the highest temperatures. Lineages A1 and A3 showed lowest and similar λ, and a relatively weak response to temperature. Bootstrapped datasets were used to obtain measures of uncertainty in population growth rates. Despite the considerable amount of variation in asymptotic growth rates (Supporting Information Figure S16 in Appendix S11), lineage L has the highest thermal tolerance in the majority of the cases. In 96%, 98%, 95% and

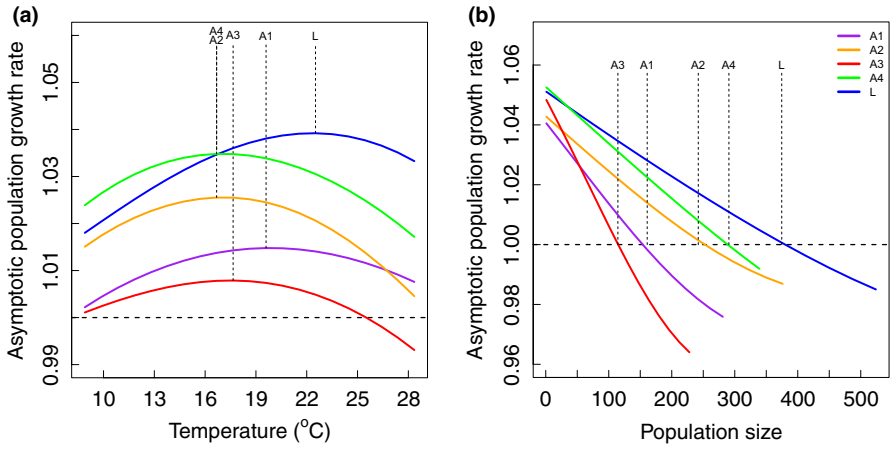

FIGURE 2 Population growth rate (λ) as a function of (a) temperature and (b) population size. In (a), population size is set at average; in (b), temperature is set at average. Each colour indicates a different lineage. See Supporting Information Appendix S11 for results taking into account uncertainty in vital rate estimates

83% of the cases, lineage L showed a higher population growth rate at the highest temperature, compared to lineages A1, A2, A3 and A4, respectively. A thermal optimum was within the range of tested temperatures in 62% (lineage L) to 86% (lineage A2) of the bootstraps, which suggests the presence of thermal optima in population growth rates. When looking at all pairwise combinations of lineage L and each other lineage, in 55% of the comparisons both lineages showed a temperature optimum within the tested temperature range. Within this subset, the temperature optimum of lineage L was higher than that of A1, A2, A3 and A4, in 78%, 89%, 79% and 90% of the cases.

All lineages show a decline in λ with increasing density, with lineage A3 suffering the most from increasing densities (Figure 2b). Ordering the lineages by the density at which λ dropped below 1 matched to a large extent with the order of observed maximum population sizes (Figure 2b). This resulted in the lowest equilibrium population sizes for lineage A3 and A1. Using the bootstrapped datasets, we evaluated uncertainty in population-level density effects. Population growth rates decreased with increasing density in 99% of the bootstraps, providing strong evidence for negative density dependence (Supporting Information Figure S17). In 91% of the bootstraps, the carrying capacity was within the range of observed population sizes. Evaluating all pairwise combinations, lineage A3 showed the lowest carrying capacity in 96% of all pairwise comparisons, while lineage L had the highest carrying capacity in 88% of all pairwise comparisons.

Using all observed population sizes during the experiment to project population growth rates, variation in density explained 60% of the variation in λ (Figure 3), followed by lineage (27%). Variation in temperature explained only 9% of the variation in λ, indicating that thermal responses in individual vital rates cancelled each other out to a considerable degree when integrated at the level of the whole population.

3.11 | Differences between lineages

Starting with an IPM which was averaged over the five lineages, and systematically replacing one of the vital rates with each of the lineage-specific vital rates, we evaluated population-level consequences of lineage differences. Different lineages realized higher population growth rates through different vital rates and none of the lineages had a demographic advantage in all vital rates (Figure 4). Results were similar when performing this analysis without lineage L (thereby changing the reference population growth rate; Supporting Information Appendix S12).

Most notable, lineage A2 benefitted from above-average survival over the complete range of temperatures (Figure 4a; Supporting Information Figure S18 in Appendix S11), but this benefit was offset by a great disadvantage in the probability of carrying eggs, especially at the high temperatures (Figure 4c–e; Supporting Information Figures S20–S22). Lineage L, in contrast, benefitted most from the vital rates related to reproduction (Figure 4c–e; Supporting Information Figure S20–S22) and had a slight disadvantage in individual growth. At last, the small differences in offspring size (Table 1) hardly contributed to differences in population growth rates among lineages (Figure 4f; Supporting Information Figure S23).

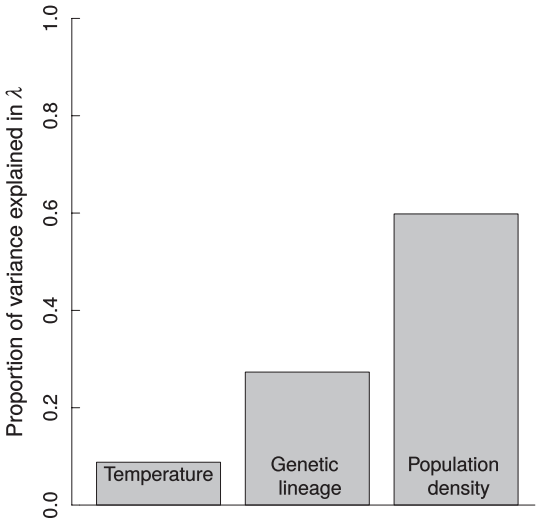

FIGURE 3 Variance explained in λ across all observed lineages, temperatures and densities. Results are based on linear regressions with one explanatory variable at a time

3.12 | Density-dependent simulation

A density-dependent simulation revealed that, after 100 days, relative abundance of the lineages changed with temperature. Overall, lineage L became more abundant at higher temperatures (Figure 5), whereas at the coldest temperatures, lineage A4 was most abundant. Lineages A2 and A4 showed the strongest decrease with increasing temperature. The proportions of lineage A1 and A3 were small and did not change much with temperature. When doing this analysis for lineage A1-A4, lineage A4 was most abundant across all temperatures. Lineages A1 and A3 out-competed lineage A2 only at the highest temperatures (Supporting Information Appendix S12).

4 | DISCUSSION

The success of a population is directly determined by the performance of its individuals. To get a more mechanistic insight into the extent to which populations can adapt towards changing environments, it is important to understand the environmental effects on separate vital rates and their integrated effect on population dynamics (Pelletier, Clutton-Brock, Pemberton, Tuljapurkar, & Coulson, 2007; Pelletier, Moyes, Clutton-Brock, & Coulson, 2012). In addition to environmental effects, the performance of individuals is simultaneously affected by many other factors, such as genotype and body size (Brooks et al., 2016; Coulson et al., 2011; Ozgul et al., 2010; Pelletier et al., 2012). Moreover, individuals may suffer from negative density-dependent processes, such as competition for food, release of chemical substances or due to physical contact, as has been

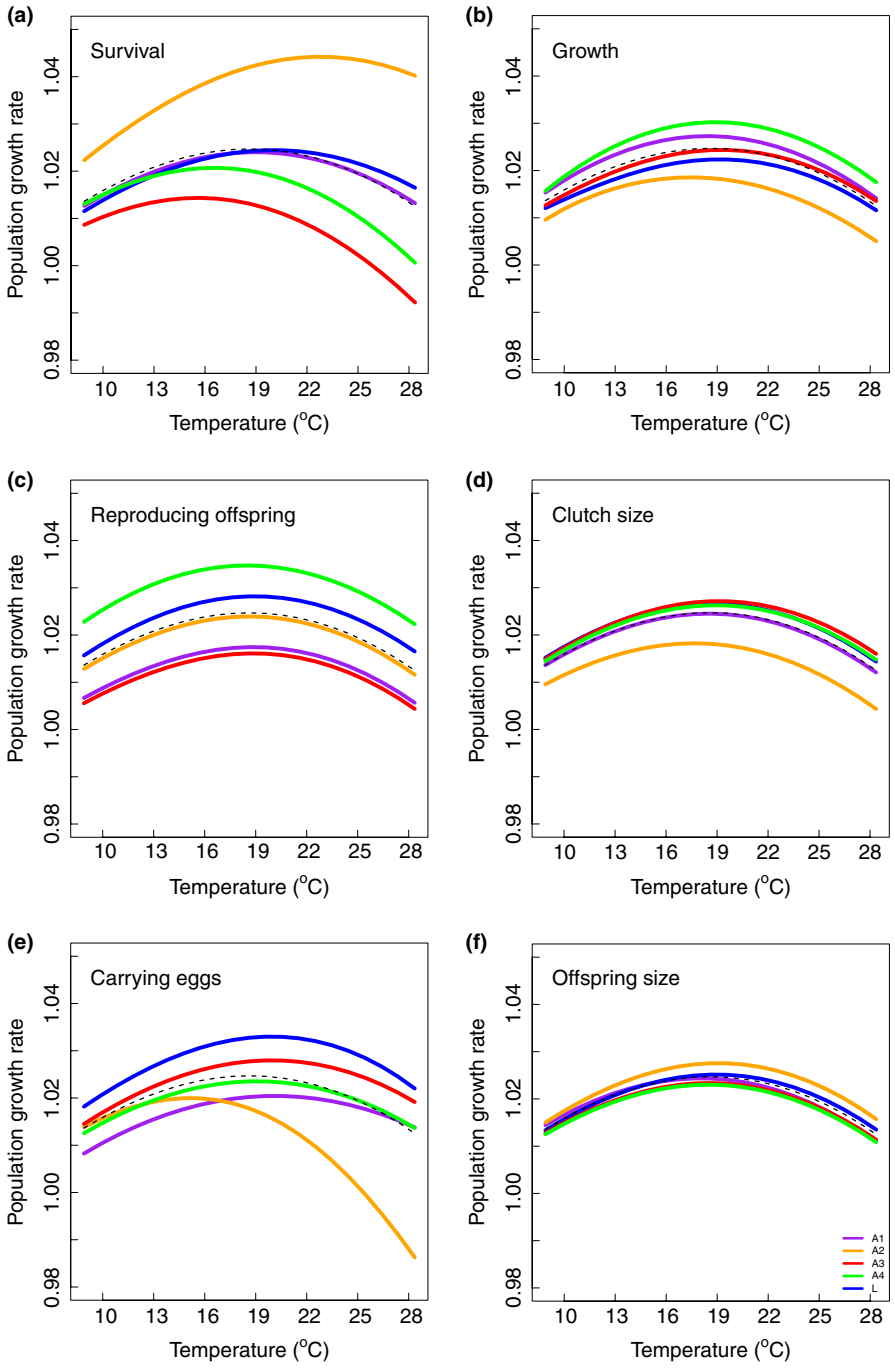

FIGURE 4 Effects on population growth rates (λ) due to differences between genetic lineages in each vital rate, compared to λ of the temperature-specific IPM averaged across lineages (dotted lines). Different colours indicate different genetic lineages. Effects were calculated by replacing one vital rate function by the corresponding vital rate function of a specific lineages and recalculate λ across the temperature range

shown in *Daphnia* (Goser & Ratte, 1994), potentially manifesting in all life-history traits.

We have studied the importance of all of the above factors, influencing population dynamics of *Daphnia magna*, via their effects on single vital rates. We have shown that *Daphnia magna* individuals embedded in populations were able to respond plastically to higher temperatures, by accelerating their life cycle, reflected by increased growth and earlier maturation. Clonal lineages showed differences in growth, survival and reproduction, and, at a population-level, responded differently to temperature (Figure 2). Results indicate trade-offs between growth, survival and reproduction, as no lineage performed the best in all vital rates (Figure 4). Our study stresses the importance of studying individuals within a population. First, following only population trends does not give information on how individuals respond and how vital rates contribute to the overall trend. Second, studying individuals without a population setting ignores density-dependent effects, which we found to have large but variable effects (Figures 2 and 3).

The structure and complexity of a population model can potentially influence results (Jongejans, Shea, Skarpaas, Kelly, & Ellner, 2011; Salguero-Gómez & Plotkin, 2010). To test the robustness of our results and ensure that our results were not driven by particular

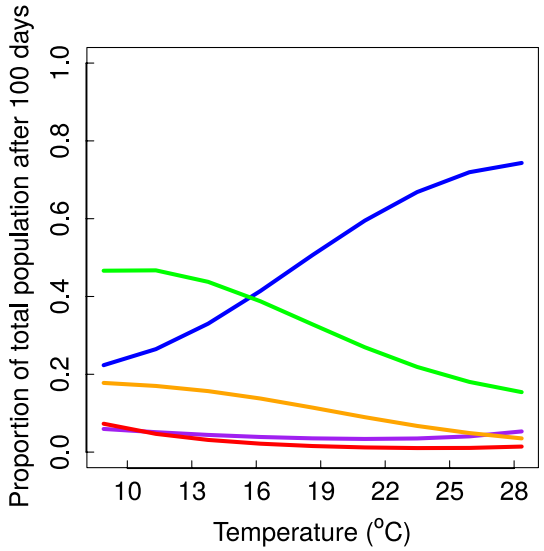

FIGURE 5 100-day density-dependent simulation of a hypothetical mixed population containing all five lineages. Each lineage started at Day 0 with four individuals. Graph shows proportion of each lineage at Day 100 over the range of temperatures (A1: purple, A2: orange, A3: red, A4: green, L: blue)

choices made to parameterize the IPM, we compared four different approaches, differing most notably in how reproduction was incorporated. As shown in Supporting Information Appendix S5, these choices resulted in similar model outcomes and hence did not affect our conclusions.

4.1 | Effects on single vital rates

Given that body size had a significant effect on all vital rates (β_1, β_4 in Table 1), understanding thermal responses requires understanding how temperature affects body size and emphasizes the importance of a trait-based approach when investigating population dynamics (Ozgul et al., 2012; Ronget, Garratt, Lemaître, & Gaillard, 2017). For all vital rates except clutch size, the best model included a temperature effect, and in four of six vital rates, this effect was significant. Individuals reared at higher temperatures became mature at a smaller size. Moreover, individuals initially grew faster, but this effect reversed at larger sizes. These plastic responses on growth and maturation have previously been described for *Daphnia* (Henning-Lucass et al., 2016; Mitchell & Lampert, 2000; Van Doorslaer et al., 2009) and are believed to be important in generating the temperature-size rule, which is followed by the majority of ectotherms (Atkinson, 1994, 1995). Survival was negatively affected by temperature, in agreement with previous studies (MacArthur & Baillie, 1929, but see Henning-Lucass et al., 2016).

We conclude that the found temperature effects on single vital rates are mostly in line with results from life table experiments, in which individuals are followed throughout their life. In our study, instead, we observed transitions over three or 4 days at a time. The big advantage of our set-up is that we were able to simultaneously quantify density effects. Somatic growth and reproductive output decreased with increasing densities, in agreement with previous work (Frank, Boll, & Kelly, 1957; Goser & Ratte, 1994; Guisande, 1993), and these density effects were often in the same order of magnitude as the temperature effects (compare β_2 and β_3). Survival probabilities showed a positive correlation with density, which seems surprising at first sight, but this was also found for individuals in different developmental stages of soil mites (Ozgul et al., 2012). We suspect a reverse causality for this correlation: Populations in which individuals survive better reach higher densities. We therefore decided to drop density in the survival models (as was also done in Traill et al., 2014 because of similar findings in bighorn sheep). Future studies could disentangle these relationships between density and survival by manipulating densities to remain constant at different levels (unlike the dynamic populations that were the focus here) or perhaps using flow-through systems (Giebelhausen & Lampert, 2001; Gliwicz, 1990).

4.2 | Integrating vital rates to predict population-level consequences

Integrating over all demographic rates enabled a quantification of the net result of the temperature effects on growth, survival and reproduction. Using asymptotic population growth rate as a proxy for population fitness (Metcalf & Pavard, 2007), we have shown that individuals were largely able to compensate for the increased mortality over the range of tested temperatures. Although there were only weak indications of temperature optima per vital rate, all lineages showed a thermal optimum when integrating all vital rates, ranging between 16.6 and 22.5°C.

Density had equally large effects on λ as temperature, clearly resulting in a carrying capacity for all lineages, and explained considerably more of the variation in daily growth rates than temperature. Furthermore, density-dependent effects differed in strength among the lineages. This, together with the stochastic component of population dynamics, would complicate direct usage of performance of isolated individuals for parameterizing population models, as was done for instance by Sommer et al. (2016). Future research will have to show under what circumstances and with which assumptions the wealth of life table experiments (that efficiently study the effects of various environmental factors on performance in isolation) can be properly scaled up to population dynamics.

Population models for zooplankton populations are rare, because it is difficult to collect demographic data on individuals embedded in the population (Jiménez-Melero, Ramírez, & Guerrero, 2013), as individuals cannot easily be marked or recognized. To overcome this, earlier studies have used "inverse" methods to estimate vital rates using data on population abundances and structure over time (Jiménez-Melero et al., 2013). This is, however, a complex problem as many combinations of vital rates can result in the same dynamics (Wood, 1994). Temporarily caging individuals in tubes enabled us to collect individual data to parameterize population models. Several factors, however, could in theory have led to differences in individual performance inside and outside the tubes. First, isolated individuals experienced a larger

volume-per-individual medium, especially at higher densities, which could have led to differences in food access (despite the use of permeable filters). Second, they did not experience physical contact with other individuals, and, finally, they had less freedom to move. To what extent these factors may have influenced the isolated individuals remains to be investigated. However, individuals were isolated for only three or 4 days, which is short compared to their life span. Moreover, the observed density effects were both convincing and remarkable; vital rates were estimated using observations on the isolated individuals, while density estimates were obtained from completely independent video analysis on the entire population. At last, ordering the lineages by their predicted carrying capacity, based on the IPMs, matched almost perfectly with the maximum observed population sizes (Figure 2). This gives confidence in our methods and results.

4.3 | Interclonal differences and life-history strategies

Individuals hatched from sexual dormant eggs differ in their genetic makeup, which can lead to differences in performance. We found clear lineage effects on vital rates, propagating to the population level. In general, lineage L showed highest population fitness over the range of tested temperatures, in particular for the higher temperatures. The overall best performance of lineage L is perhaps not surprising, as this lineage has been successfully held in the laboratory for more than 10 years (Lürling & Tolman, 2010), thereby having proved its ability to perform well under laboratory settings. In contrast, the other four lineages (A1-A4) were used only 1 year after hatching from dormant eggs collected in the field. Model species such as *Daphnia magna* play a central role in climate change research. However, our results warn against extrapolating conclusions based on lineages that have been raised and selected to do well under laboratory conditions, as these may not be representative for natural populations.

Within-population variation in vital rates and population-level responses has been demonstrated in *Daphnia* (Carvalho, 1987; Jansen, Coors, Stoks, & De Meester, 2011; Pantel, Duvivier, & De Meester, 2015; Pietrzak, 2011; Stoks, Govaert, Pauwels, Jansen, & De Meester, 2016; Van Doorslaer et al., 2009) and is in agreement with our results. When comparing lineage A1-A4, the differential life-history strategies suggest that there is substantial within-population variation for natural selection to act upon (see also Van Doorslaer et al., 2009, 2010). Differentiation in thermal tolerance among lineages (Mitchell & Lampert, 2000) may indicate the presence of seasonal clones, which are adapted to specific periods of the growing season (Carvalho, 1987). As no lineage out-competed other lineages in all vital rates, our results suggest trade-offs between survival, growth and reproduction, in accordance with Dudycha and Tessier (1999) and Reznick, Nunney, and Tessier (2000). It is interesting that we have shown that these trade-offs between multiple vital rates were meaningful in a population context and that different clonal lineages maximized their fitness via different routes (e.g. De Meester, Weider, & Tollrian, 1995).

4.4 | Evolutionary potential for thermal adaptation

We used integral projection models to make testable predictions on evolutionary change and predicted that, after only 100 days, the genetic composition of a mixed population can be substantially altered due to interclonal fitness differences and that these changes are temperature-dependent. These predictions, based on the performance of single lineages, are yet to be tested. This could be done by following populations consisting of two or more lineages, while following the abundance of each lineage, for instance using genetic markers (Turcotte, Reznick, & Hare, 2011). Discrepancies between predicted and observed evolutionary changes could indicate that the presence of other genotypes has differential effects on the performance of individuals, compared to density effects of individuals of the same lineage.

The role of evolution in short-term adaptive trait changes is recently receiving much attention (van Benthem et al., 2017; Ellner, Geber, & Hairston, 2011; Pelletier et al., 2009; Schoener, 2011), and rapid evolutionary responses have now been shown in many experimental systems (e.g. Becks, Ellner, Jones, & Hairston, 2012; Cameron, O'Sullivan, Reynolds, Piertney, & Benton, 2013; Turcotte, Reznick, & Daniel Hare, 2013). In *Daphnia*, thermal evolution experiments have shown rapid adaptive responses towards changing temperatures (Geerts et al., 2015; Van Doorslaer et al., 2009, 2010), and this evolutionary potential for thermal adaptation is supported by our results. Our work differs from earlier studies in that we quantified thermal responses by integrating all fitness components to obtain estimates of population growth rate as a proxy for fitness, which is the metric that is optimized by natural selection. From a population adaptation perspective, this gives a more complete picture compared to studies documenting thermal responses in single fitness components such as somatic growth (Mitchell & Lampert, 2000) or maximum thermal tolerance (CT_{max}; Geerts et al., 2015). Moreover, when obtaining these fitness components from single individuals, information on the interplay between density, the environment and genetic background, and integrated effects of all vital rates is lacking. On the other hand, previous studies on eco-evolutionary dynamics that did focus on populations trends (Turcotte et al., 2011, 2013; Van Doorslaer et al., 2010) generally lack information on performance of individuals within the population.

As shown here, using individual demographic rates, as obtained from individuals embedded in a population, and integrating these into a population model, gives a more mechanistic understanding of population-level responses towards climate change. Moreover, density had equally large effects as temperature on vital rates and explained more of the variation in daily growth rates. We conclude that these meaningful density effects cannot safely be ignored when predicting population responses to environmental change. Future studies applying our approach to different clones or species, for example from different locations (Yampolsky, Schaer, & Ebert, 2013) or periods (Geerts et al., 2015), will greatly improve the understanding of evolutionary potential for thermal adaptation. It will also help to identify life stages whose expected demographic responses to future environmental change contribute

most to changes in population fitness. These life stages could be the most promising targets for conservation strategies. Natural populations facing climatic changes are not purely affected by the changes in temperature, but also by associated changes in for instance densities, food availability and pathogen dynamics. Scaling our technique of quantifying demography on temporarily partially isolated individuals up to mesocosm or field studies will provide novel insights into eco-evolutionary responses to climate change in a more natural setting. Together with other types of "evo-demo" studies (Ronget et al., 2017), our approach should lead to enhanced understanding of how much resilience we can expect due to phenotypic plasticity and rapid evolution on relevant short time-scales, when assessing the vulnerability of animal communities to the effects of global change.

ACKNOWLEDGEMENTS

We are grateful to Luc De Meester, Wilco Verberk, Marco Visser and Sarian Kosten for comments on earlier versions of this manuscript. We thank Wendy Beekman-Lukassen from Wageningen University for kindly providing the *Daphnia magna* clone (lineage L) and Martin Soesbergen for informing us on where *Daphnia magna* occurs in the Netherlands, and we thank Tom Spanings for practical help. We thank two anonymous reviewers for helpful comments and suggestions. The authors have no conflict of interest to declare.

AUTHOR'S CONTRIBUTIONS

M.B. and E.J. conceived the ideas and designed methodology; A.C.M.B. and M.B. collected the data; M.B. analysed the data; M.B. led the writing of the manuscript. All authors contributed critically to the drafts and gave final approval for publication.

DATA ACCESSIBILITY

Data are archived in the DANS EASY repository (https://doi.org/10.17026/dans-2b8-gx7j).

ORCID

Marjolein Bruijning http://orcid.org/0000-0002-9408-2187
Eelke Jongejans http://orcid.org/0000-0003-1148-7419

REFERENCES

Atkinson, D. (1994). Temperature and organism size—a biological law for ectotherms? *Advances in Ecological Research*, *25*, 1–58.

Atkinson, D. (1995). Effects of temperature on the size of aquatic ectotherms: Exceptions to the general rule. *Journal of Thermal Biology*, *20*, 61–74. https://doi.org/10.1016/0306-4565(94)00028-H

Bartoń, K. (2016). MuMIn: Multi-Model Inference. R package version 1.15.6. Retrieved from https://CRAN.R-project.org/package=MuMIn

Becks, L., Ellner, S. P., Jones, L. E., & Hairston, N. G. (2012). The functional genomics of an eco-evolutionary feedback loop: Linking gene expression, trait evolution, and community dynamics. *Ecology Letters*, *15*, 492–501. https://doi.org/10.1111/j.1461-0248.2012.01763.x

van Benthem, K. J., Bruijning, M., Bonnet, T., Jongejans, E., Postma, E., & Ozgul, A. (2017). Disentangling evolutionary, plastic and demographic processes underlying trait dynamics: A review of four frameworks. *Methods in Ecology and Evolution*, *8*, 75–85. https://doi.org/10.1111/2041-210X.12627

Brooks, M. E., Mugabo, M., Rodgers, G. M., Benton, T. G., & Ozgul, A. (2016). How well can body size represent effects of the environment on demographic rates? Disentangling correlated explanatory variables. *Journal of Animal Ecology*, *85*, 318–328. https://doi.org/10.1111/1365-2656.12465

Bruijning, M., ten Berge, A., & Jongejans, E. (2018a). Data for: Population-level responses to temperature, density and clonal differences in Daphnia magna as revealed by Integral Projection Modeling. DANS EASY Archive (https://doi.org/10.17026/dans-2b8-gx7j).

Bruijning, M., Visser, M. D., Hallmann, C. A., & Jongejans, E. (2018b). trackdem: Automated particle tracking to obtain population counts and size distributions from videos in R. *Methods in Ecology and Evolution*, *9*, 965–973. https://doi.org/10.1111/2041-210X.12975

Burnham, K. P., & Anderson, D. R. (2002). *Model selection and multi-model inference: A practical information-theoretic approach*. Berlin, Germany: Springer.

Burnham, K. P., & Anderson, D. R. (2004). Multimodel Inference Understanding AIC and BIC in Model Selection. *Sociological Methods and Research*, *33*, 261–304. https://doi.org/10.1177/0049124104268644

Cameron, T. C., O'Sullivan, D., Reynolds, A., Piertney, S. B., & Benton, T. G. (2013). Eco-evolutionary dynamics in response to selection on life-history. *Ecology Letters*, *16*, 754–763. https://doi.org/10.1111/ele.12107

Carvalho, G. R. (1987). The clonal ecology of *Daphnia magna* (Crustacea: Cladocera): II. Thermal differentiation among seasonal clones. *Journal of Animal Ecology*, *56*, 469–478. https://doi.org/10.2307/5061

Chevin, L. M. (2015). Evolution of adult size depends on genetic variance in growth trajectories: A comment on analyses of evolutionary dynamics using integral projection models. *Methods in Ecology and Evolution*, *6*, 981–986. https://doi.org/10.1111/2041-210X.12389

Chevin, L. M., Collins, S., & Lefèvre, F. (2013). Phenotypic plasticity and evolutionary demographic responses to climate change: Taking theory out to the field. *Functional Ecology*, *27*, 967–979. https://doi.org/10.1111/j.1365-2435.2012.02043.x

Colbourne, J. K., Pfrender, M. E., & Gilbert, D. (2011). The ecoresponsive genome of *Daphnia pulex*. *Science*, *331*, 555–561. https://doi.org/10.1126/science.1197761

Coulson, T., MacNulty, D. R., Stahler, D. R., Wayne, R. K., & Smith, D. W. (2011). Modeling effects of environmental change on wolf population dynamics, trait evolution, and life history. *Science*, *334*, 1275–1278. https://doi.org/10.1126/science.1209441

De Meester, L., Van Doorslaer, W., Geerts, A., Orsini, L., & Stoks, R. (2011). Thermal genetic adaptation in the water flea *Daphnia* and its impact: An evolving metacommunity approach. *Integrative and Comparative Biology*, *51*, 703–718. https://doi.org/10.1093/icb/icr027

De Meester, L., Weider, L. J., & Tollrian, R. (1995). Alternative antipredator defenses and genetic-polymorphism in a pelagic predator-prey system. *Nature*, *378*, 483–485. https://doi.org/10.1038/378483a0

Duchet, C., Coutellec, M.-A., Franquet, E., Lagneau, C., & Lagadic, L. (2010). Population-level effects of spinosad and *Bacillus thuringiensis israelensis* in *Daphnia pulex* and *Daphnia magna*: Comparison of laboratory and field microcosm exposure conditions. *Ecotoxicology*, *19*, 1224–1237. https://doi.org/10.1007/s10646-010-0507-y

Dudycha, J. L., & Tessier, A. J. (1999). Natural genetic variation of life span, reproduction, and juvenile growth in *Daphnia*. *Evolution*, *53*, 1744–1756. https://doi.org/10.1111/j.1558-5646.1999.tb04559.x

Ellner, S. P., Childs, D. Z., & Rees, M. (2016). *Data-driven modelling of structured populations. A practical guide to the integral projection model*. Berlin, Germany: Springer International Publishing. https://doi.org/10.1007/978-3-319-28893-2

Ellner, S. P., Geber, M. A., & Hairston, N. G. (2011). Does rapid evolution matter? Measuring the rate of contemporary evolution and its impacts on ecological dynamics. *Ecology Letters*, *14*, 603–614. https://doi.org/10.1111/j.1461-0248.2011.01616.x

Ellner, S. P., & Rees, M. (2006). Integral projection models for species with complex demography. *American Naturalist*, *167*, 410–428. https://doi.org/10.1086/499438

Frank, P., Boll, C., & Kelly, R. (1957). Vital statistics of laboratory cultures of *Daphnia pulex* DeGeer as related to density. *Physiological Zoology*, *30*, 287–305. https://doi.org/10.1086/physzool.30.4.30152211

Gabsi, F., Glazier, D. S., Hammers-Wirtz, M., Ratte, H. T., & Preuss, T. G. (2014). How do interactive maternal traits and environmental factors determine offspring size in *Daphnia magna*? *International Journal of Limnology*, *50*, 9–18. https://doi.org/10.1051/limn/2013067

Geerts, A. N., Vanoverbeke, J., Vanschoenwinkel, B., Van Doorslaer, W., Feuchtmayr, H., Atkinson, D., … De Meester, L. (2015). Rapid evolution of thermal tolerance in the water flea *Daphnia*. *Nature Climate Change*, *5*, 665–668. https://doi.org/10.1038/nclimate2628

Giebelhausen, B., & Lampert, W. (2001). Temperature reaction norms of Daphnia magna: The effect of food concentration. *Freshwater Biology*, *46*, 281–289. https://doi.org/10.1046/j.1365-2427.2001.00630.x

Gienapp, P., Teplitsky, C., Alho, J. S., Mills, J. A., & Merilä, J. (2008). Climate change and evolution: Disentangling environmental and genetic responses. *Molecular Ecology*, *17*, 167–178. https://doi.org/10.1111/j.1365-294X.2007.03413.x

Gliwicz, Z. M. (1990). Food thresholds and body size in cladocerans. *Nature*, *343*, 638. https://doi.org/10.1038/343638a0

Goser, B., & Ratte, H. T. (1994). Experimental evidence of negative interference in *Daphnia magna*. *Oecologia*, *98*, 354–361. https://doi.org/10.1007/BF00324224

Grueber, C. E., Nakagawa, S., Laws, R. J., & Jamieson, I. G. (2011). Multimodel inference in ecology and evolution: Challenges and solutions. *Journal of Evolutionary Biology*, *24*, 699–711. https://doi.org/10.1111/j.1420-9101.2010.02210.x

Guisande, C. (1993). Reproductive strategy as population density varies in *Daphnia magna* (Cladocera). *Freshwater Biology*, *29*, 463–467. https://doi.org/10.1111/j.1365-2427.1993.tb00780.x

Gust, K. A., Kennedy, A. J., Melby, N. L., Wilbanks, M. S., Laird, J., Meeks, B., … Perkins, E. J. (2016). Daphnia magna's sense of competition: Intra-specific interactions (ISI) alter life history strategies and increase metals toxicity. *Ecotoxicology*, *25*, 1126–1135. https://doi.org/10.1007/s10646-016-1667-1

Hairston, N. G., Lampert, W., Cáceres, C. E., Holtmeier, C. L., Weider, L. J., Gaedke, U., … Post, D. M. (1999). Lake ecosystems: Rapid evolution revealed by dormant eggs. *Nature*, *401*, 446. https://doi.org/10.1038/46731

Henning-Lucass, N., Cordellier, M., Streit, B., & Schwenk, K. (2016). Phenotypic plasticity in life-history traits of Daphnia galeata in response to temperature–a comparison across clonal lineages separated in time. *Ecology and Evolution*, *6*, 881–891. https://doi.org/10.1002/ece3.1924

Hoefnagel, K. N., de Vries, E. H. J. L., Jongejans, E., & Verberk, W. C. E. P. (2018). The temperature-size rule in *Daphnia magna* across different genetic lines and ontogenetic stages: Multiple patterns and mechanisms. *Ecology and Evolution*, *8*, 3828–3841. https://doi.org/10.1002/ece3.3933

Hoeting, J. A., Madigan, D., Raftery, A. E., & Volinsky, C. T. (1999). Bayesian model averaging: A tutorial. *Source: Statistical Science*, *Statistical Science*, *14*, 382–401.

Hoffmann, A. A., & Sgrò, C. M. (2011). Climate change and evolutionary adaptation. *Nature*, *470*, 479–485. https://doi.org/10.1038/nature09670

Huey, R., & Berrigan, D. (2001). Temperature, demography, and ectotherm fitness. *American Naturalist*, *158*, 204–210. https://doi.org/10.1086/321314

Jansen, M., Coors, A., Stoks, R., & De Meester, L. (2011). Evolutionary ecotoxicology of pesticide resistance: A case study in *Daphnia*. *Ecotoxicology*, *20*, 543–551. https://doi.org/10.1007/s10646-011-0627-z

Jaqaman, K., Loerke, D., Mettlen, M., Kuwata, H., Grinstein, S., Schmid, S. L., & Danuser, G. (2008). Robust single-particle tracking in live-cell time-lapse sequences. *Nature Methods*, *5*, 695–702. https://doi.org/10.1038/nmeth.1237

Jiménez-Melero, R., Ramírez, J. M., & Guerrero, F. (2013). Seasonal variation in the population growth rate of a dominant zooplankter: What determines its population dynamics? *Freshwater Biology*, *58*, 1221–1233. https://doi.org/10.1111/fwb.12122

Jongejans, E., Shea, K., Skarpaas, O., Kelly, D., & Ellner, S. P. (2011). Importance of individual and environmental variation for invasive species spread: A spatial integral projection model. *Ecology*, *92*, 86–97. https://doi.org/10.1890/09-2226.1

Kingsolver, J. G., & Huey, R. B. (2008). Size, temperature, and fitness: Three rules. *Evolutionary Ecology Research*, *10*, 251–268.

Kleiven, O. T., Larsson, P., & Hobæk, A. (1992). Sexual reproduction in Daphnia magna requires three stimuli. *Oikos*, *65*, 197–206. https://doi.org/10.2307/3545010

de Kroon, H., van Groenendael, J., & Ehrlén, J. (2000). Elasticities: A review of methods and model limitations. *Ecology*, *81*, 607–618. https://doi.org/10.1890/0012-9658(2000)081[0607:EAROMA]2.0.CO;2

Lavergne, S., Mouquet, N., Thuiller, W., & Ronce, O. (2010). Biodiversity and climate change: Integrating evolutionary and ecological responses of species and communities. *Annual Review of Ecology, Evolution and Systematics*, *41*, 321–350. https://doi.org/10.1146/annurev-ecolsys-102209-144628

Lukacs, P. M., Burnham, K. P., Anderson, D. R., Lukacs, P. M., Burnham, K. P., & Anderson, D. R. (2010). Model selection bias and Freedman's paradox. *Annals of the Institute of Statistical Mathematics*, *62*, 117–125. https://doi.org/10.1007/s10463-009-0234-4

Lürling, M., & Tolman, Y. (2010). Effects of lanthanum and lanthanum-modified clay on growth, survival and reproduction of *Daphnia magna*. *Water Research*, *44*, 309–319. https://doi.org/10.1016/j.watres.2009.09.034

MacArthur, J. W., & Baillie, W. H. T. (1929). Metabolic activity and duration of life. I. Influence of temperature on longevity in *Daphnia magna*. *Journal of Experimental Zoology*, *53*, 221–242. https://doi.org/10.1002/(ISSN)1097-010X

Madigan, D., & Raftery, A. E. (1994). Model Selection and Accounting for Model Uncertainty in Graphical Models Using Occam's Model Selection and Accounting for Model Uncertainty in Graphical Models Using Occam's Window. *Source Journal of the American Statistical Association*, *89*, 1535–1546. https://doi.org/10.1080/01621459.1994.10476894

McLean, N., Lawson, C. R., Leech, D. I., & Pol, M. (2016). Predicting when climate-driven phenotypic change affects population dynamics. *Ecology Letters*, *19*, 595–608. https://doi.org/10.1111/ele.12599

Metcalf, C. J. E., & Pavard, S. (2007). Why evolutionary biologists should be demographers. *Trends in Ecology and Evolution*, *22*, 205–212. https://doi.org/10.1016/j.tree.2006.12.001

Mitchell, S. E., & Lampert, W. (2000). Temperature adaptation in a geographically widespread zooplankter, *Daphnia magna*. *Journal of Evolutionary Biology*, *13*, 371–382. https://doi.org/10.1046/j.1420-9101.2000.00193.x

NEN6503 (1980). Methodebeschrijvingen voor de beoordeling van verontreinidgde waterbodems volgens de TRIADE benadering.

Ozgul, A., Childs, D. Z., Oli, M. K., Armitage, K. B., Blumstein, D. T., Olson, L. E., … Coulson, T. (2010). Coupled dynamics of body mass

and population growth in response to environmental change. *Nature*, *466*, 482–485. https://doi.org/10.1038/nature09210

Ozgul, A., Coulson, T., Reynolds, A., Cameron, T. C., & Benton, T. G. (2012). Population responses to perturbations: The importance of trait-based analysis illustrated through a microcosm experiment. *American Naturalist*, *179*, 582–594. https://doi.org/10.1086/664999

Pantel, J. H., Duvivier, C., & De Meester, L. (2015). Rapid local adaptation mediates zooplankton community assembly in experimental mesocosms. *Ecology Letters*, *18*, 992–1000. https://doi.org/10.1111/ele.12480

Pelletier, F., Clutton-Brock, T., Pemberton, J., Tuljapurkar, S., & Coulson, T. (2007). The evolutionary demography of ecological change: Linking trait variation and population growth. *Science*, *315*, 1571–1574. https://doi.org/10.1126/science.1139024

Pelletier, F., Garant, D., & Hendry, A. P. (2009). Eco-evolutionary dynamics. *Philosophical Transactions of the Royal Society B: Biological Sciences*, *364*, 1483–1489. https://doi.org/10.1098/rstb.2009.0027

Pelletier, F., Moyes, K., Clutton-Brock, T. H., & Coulson, T. (2012). Decomposing variation in population growth into contributions from environment and phenotypes in an age-structured population. *Proceedings of the Royal Society of London B: Biological Sciences*, *279*, 394–401. https://doi.org/10.1098/rspb.2011.0827

Pietrzak, B. (2011). Interclonal differences in age-specific performance in *Daphnia magna*. *Journal of Limnology*, *70*, 345–352. https://doi.org/10.4081/jlimnol.2011.345

R Core Team (2016) *R: A language and environment for statistical computing*. Vienna, Austria: R Core Team.

Raftery, A. E., Madigan, D., & Hoeting, J. A. (1997). Bayesian model averaging for linear regression models. *Journal of the American Statistical Association*, *92*, 179–191. https://doi.org/10.1080/01621459.1997.10473615

Reznick, D., Nunney, L., & Tessier, A. (2000). Big houses, big cars, superfleas and the costs of reproduction. *Trends in Ecology and Evolution*, *15*, 421–425. https://doi.org/10.1016/S0169-5347(00)01941-8

Ronget, V., Garratt, M., Lemaître, J.-F., & Gaillard, J.-M. (2017). The "Evo-Demo" Implications of Condition-Dependent Mortality. *Trends in ecology & evolution*, *32*, 909–921. https://doi.org/10.1016/j.tree.2017.09.003

Salguero-Gómez, R., & Plotkin, J. B. (2010). Matrix dimensions bias demographic inferences: Implications for comparative plant demography. *American Naturalist*, *176*, 710–722. https://doi.org/10.1086/657044

Schoener, T. W. (2011). The newest synthesis: Understanding the interplay of evolutionary and ecological dynamics. *Science*, *331*, 426–429. https://doi.org/10.1126/science.1193954

Smallegange, I. M., & Coulson, T. (2013). Towards a general, population-level understanding of eco-evolutionary change. *Trends in Ecology and Evolution*, *28*, 143–148. https://doi.org/10.1016/j.tree.2012.07.021

Sommer, S., Piscia, R., Manca, M. M., Fontaneto, D., & Ozgul, A. (2016). Demographic cost and mechanisms of adaptation to environmental stress in resurrected Daphnia. *Journal of Limnology*, *75*, 30–35.

Stearns, S. C. (1989). Trade-offs in life-history evolution. *Functional Ecology*, *3*, 259–268. https://doi.org/10.2307/2389364

Stoks, R., Govaert, L., Pauwels, K., Jansen, B., & De Meester, L. (2016). Resurrecting complexity: The interplay of plasticity and rapid evolution in the multiple trait response to strong changes in predation pressure in the water flea *Daphnia*. *Ecology Letters*, *19*, 180–190. https://doi.org/10.1111/ele.12551

Traill, L. W., Schindler, S., & Coulson, T. (2014). Demography, not inheritance, drives phenotypic change in hunted bighorn sheep. *Proceedings of the National Academy of Sciences of the USA*, *111*, 13223–13228. https://doi.org/10.1073/pnas.1407508111

Turcotte, M. M., Reznick, D. N., & Daniel Hare, J. (2013). Experimental test of an eco-evolutionary dynamic feedback loop between evolution and population density in the green peach aphid. *American Naturalist*, *181*, S46–S57. https://doi.org/10.1086/668078

Turcotte, M. M., Reznick, D. N., & Hare, J. D. (2011). The impact of rapid evolution on population dynamics in the wild: Experimental test of eco-evolutionary dynamics. *Ecology Letters*, *14*, 1084–1092. https://doi.org/10.1111/j.1461-0248.2011.01676.x

Van Doorslaer, W., Stoks, R., Duvivier, C., Bednarshka, A., & De Meester, L. (2009). Population dynamics determine genetic adaptation to temperature in *Daphnia*. *Evolution*, *63*, 1867–1878. https://doi.org/10.1111/j.1558-5646.2009.00679.x

Van Doorslaer, W., Stoks, R., Swillen, I., Feuchtmayr, H., Atkinson, D., Moss, B., & De Meester, L. (2010). Experimental thermal microevolution in community-embedded *Daphnia* populations. *Climate Research*, *43*, 81–89. https://doi.org/10.3354/cr00894

Villellas, J., Doak, D. F., García, M. B., & Morris, W. F. (2015). Demographic compensation among populations: What is it, how does it arise and what are its implications? *Ecology Letters*, *18*, 1139–1152. https://doi.org/10.1111/ele.12505

Wood, S. N. (1994). Obtaining birth and mortality patterns from structured population trajectories. *Ecological Monographs*, *64*, 23–44. https://doi.org/10.2307/2937054

Yampolsky, L. Y., Schaer, T. M. M., & Ebert, D. (2013). Adaptive phenotypic plasticity and local adaptation for temperature tolerance in freshwater zooplankton. *Proceedings of the Royal Society of London B: Biological Sciences*, *281*, 20132744. https://doi.org/10.1098/rspb.2013.2744

Yang, Y. (2007). Prediction/Estimation with simple linear models: Is it really that simple? *Econometric Theory*, *23*, 1–36.

SUPPORTING INFORMATION

Additional supporting information may be found online in the Supporting Information section at the end of the article.

How to cite this article: Bruijning M, ten Berge ACM, Jongejans E. Population-level responses to temperature, density and clonal differences in *Daphnia magna* as revealed by integral projection modelling. *Funct Ecol*. 2018;32:2407–2422. https://doi.org/10.1111/1365-2435.13192